Int. J. Heat Mass Transfer. Vol. 27, No. 9, pp. 1445–1453, 1984
Printed in Great Britain

0017-9310/84 $3.00 + 0.00

An interferometric study of the natural convection in an inclined water layer

R. J. GOLDSTEIN and Q.-J. WANG
Mechanical Engineering Department, University of Minnesota, Minneapolis, MN 55455, U.S.A.

(*Received* 12 *December* 1983)

Abstract—Thermal instability and heat transfer by natural convection in an inclined rectangular water layer at low Rayleigh number have been studied using an interferometer. At different angles of inclination to the horizontal (θ) different preferred flow modes are observed. For $0° < \theta < 57.5°$, the preferred mode is longitudinal rolls superimposed on the base flow. For $57.5° \leqslant \theta \leqslant 90°$ a single two-dimensional roll is observed. Measured local and average Nusselt numbers are compared to numerical solutions carried out assuming a two-dimensional transverse roll.

INTRODUCTION

BUOYANCY driven instability and convective motion in differentially-heated inclined enclosures is of interest in a number of engineering applications, including solar heating and nuclear reactor design and safety. The preferred mode of circulation, the criteria for the onset of convection and the heat transfer across enclosures of fluid have received extensive study.

Hart [1] carried out an early systematic study using air and water in enclosures with nominal aspect ratios ($AX = W/H$) of 36 and 25. Using dye injected at strategic locations in the fluid he observed both longitudinal and transverse rolls. The transition from three- to two-dimensional (3- to 2-D) flow was found to occur at an inclination of the layer to the horizontal of about 80°.

Hollands and Konicek [2] determined the critical Rayleigh numbers in a layer of air with a nominal aspect ratio of 44 and highly conducting ends. From changes in the heat flux they found a transition angle (a crossover from one class of flow to the other) of 75°.

Pellow and Southwell [3] considered the effects of finite aspect ratio on instability in a horizontal layer. When a fluid is constrained laterally, the required critical temperature gradient is increased. If the layer of fluid is a rectangular parallelepiped, aspect ratios, AX and AZ, based on both horizontal dimensions influence the instability. Catton [4] derived an approximate correlation in which the critical Rayleigh number is a function of the two aspect ratios AX and AZ.

Ozoe *et al.* [5] measured heat transfer across an inclined square channel ($AX = 1$, $AZ = 18$) for $\theta = 0°$–$90°$ at $Ra = 3800$, 4950, and 11 000; glycerol ($Pr = 2690$–5580) was the test fluid. At a fixed Rayleigh number a minimum in the Nusselt number was observed at $\theta \simeq 5°$. The minimum is presumed to be due to a transition between two different flow patterns. In a subsequent paper, Ozoe [6] reported experimental results for $\theta = 0°$–$180°$ for convection channels ($AX = 3$ and $AZ = 12$) with $Ra = 4770$ and $Pr = 4045$. The minimum in Nu occurred in the neighborhood of 25°. In a third paper, Ozoe *et al.* [7] used channels in which AX was 1, 2, 3, 4.2, 8.4, and 15.5; the corresponding values of AZ were 5.85, 11.23, 12.12, 12.63, 8.40, and 15.5, respectively. Silicone oil was used in the four channels of smallest aspect ratio; air was used in the others. They found that the transition angle as determined by the minimum in Nu is a strong function of the aspect ratio AX and a weak function of the Rayleigh number.

Arnold *et al.* [8] reported experimental results for an enclosure with AX of 1, 3, 6, and 12 and AZ of 9.87. Water and silicone oil (50–200 cs) were used as test fluids; the Prandtl number range was from 4.5 to 2000; and θ varied from 0° to 180°. They obtained transition angles for the different channels and for $Ra > 10^4$ they provided a heat transfer correlation. For $Ra < 10^4$ the variation of Nu with Ra did not obey a power law. The angle of inclination at which the minimum in heat transfer occurred was considerably greater (25° vs 5° at $AX = 1$ and 45° vs 25° at $AX = 3$) than that reported in refs. [6, 7]. This was attributed to differences in the value of the Rayleigh number.

Recently, Linthorst *et al.* [9] determined the transition from 2- to 3-D flow in an inclined enclosure. They found no significant effect of Ra on the transition angle particularly for nominal aspect ratios of 1, 4, and 7.

Korpela [10] investigated the effect of Prandtl number on stability in an inclined slot. He indicated that for a very large nominal aspect ratio the transition angle increases from 1° to 90° as the Prandtl number decreases from 12.7 to 0.24. Elsherbiny *et al.* [11] investigated the effect of thermal boundary conditions on natural convection in inclined air layers.

It appears that the preferred mode of circulation and the criteria for the onset of convection in inclined enclosures are still not completely known. It is clear that there are numerous influential parameters, such as Rayleigh number, Prandtl number, variation of physical properties with temperature, the two aspect ratios, and thermal and flow boundary conditions.

Reviews of experimental studies of overall heat flow

NOMENCLATURE

AX	nominal (width) aspect ratio—see Fig. 1 (9.25 in the present study), W/H
AZ	depth aspect ratio—see Fig. 1 (17.2 in the present study), D/H
D	depth of experimental enclosure in z-direction
g	gravitational acceleration
h_x	local heat transfer coefficient at position x averaged over z-direction
H	height of experimental enclosure in y-direction, thickness of fluid layer
Nu	Nusselt number
Nu_x	local Nusselt number, based on h_x and D
$Nu_{x,c}$	local Nusselt number on cold plate
$Nu_{x,h}$	local Nusselt number on hot plate
$\overline{Nu}$	average Nusselt number over plate surface
Pr	Prandtl number
Ra	Rayleigh number, based on $(T_h - T_c)$ and H
Ra_{cr}	critical Rayleigh number
T	temperature
T_c	temperature of cold plate surface
T_h	temperature of hot plate surface
W	width of experimental enclosure in x-direction
X	coordinate in x-direction—cf. Fig. 1
Y	coordinate in y-direction—cf. Fig. 1
Z	coordinate in z-direction which lies in a horizontal plane (enclosure pivots about z-axis)—cf. Fig. 1.

Greek symbol

θ	angle of inclination of enclosure from horizontal measured around z-axis.

across inclined enclosures are given by Buchberg *et al.* [12] and Catton [13]. Most investigators used air in the layer. Recently, Elsherbiny *et al.* [14] presented results of heat transfer measurements in inclined air layers; the separate effects of aspect ratio and Rayleigh number on the heat transfer were determined. Dropkin and Somerscales [15] presented experimental results using water, silicone oil, and mercury. Their experiments covered a large range of Ra from 5×10^4 to 7.17×10^8. In their results, a significant Prandtl number effect is reported [15]. There is little information on heat transfer across liquids in inclined enclosures in the immediate neighborhood of instability ($Ra \sim 10^3$–10^4).

In the present research, stability and heat transfer by natural convection in an inclined rectangular water enclosure are studied using interferometric techniques. Compared to measuring overall heat flow, interferometric observation can provide a more direct image of the onset of changes in flow pattern at different angles of inclination.

In the present tests the nominal aspect ratio (AX) is 9.25, and the depth aspect ratio (AZ) is 17.2. The Rayleigh number is varied between 1.7×10^3 and 4×10^4. The angle of tilt of the enclosure with respect to the horizontal covers the range from 0° to 180° (for $0° \leqslant \theta \leqslant 90°$ heated from below, for $90° < \theta \leqslant 180°$ heated from above). Water is the test medium.

As a comparison, a numerical solution is carried out using a finite-difference scheme to predict the temperature and flow fields assuming a 2-D transverse roll.

NUMERICAL SOLUTION

Figure 1 is a schematic diagram of the system geometry. We assume steady 2-D flow and neglect compressive work and viscous dissipation. The governing momentum, energy and continuity equations and boundary conditions are similar to those in ref. [16] except that the internal energy sources are equal to zero.

The set of partial differential equations has been solved by using a general purpose computer program developed for 2-D elliptic situations [17]. A 22×18 symmetrical logarithmic grid is used to assure the accuracy of the temperature gradient at the two plate surfaces. Underrelaxation is used to avoid divergence in the line-by-line iterative solution due to the nonlinear nature of the set of equations. Most cases took about 80 iterations for convergence. Figure 2 shows a set of isotherms and streamlines obtained by the computation. An interferogram taken under similar conditions is shown for comparison. The two sets of isotherms appear to be in good agreement.

THE EXPERIMENTAL SYSTEM

A schematic view of the experimental apparatus is shown in Fig. 3. The test section includes two parallel

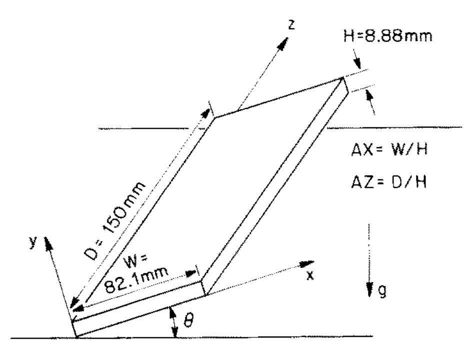

FIG. 1. Differentially heated layer inclined at an angle θ to the horizontal.

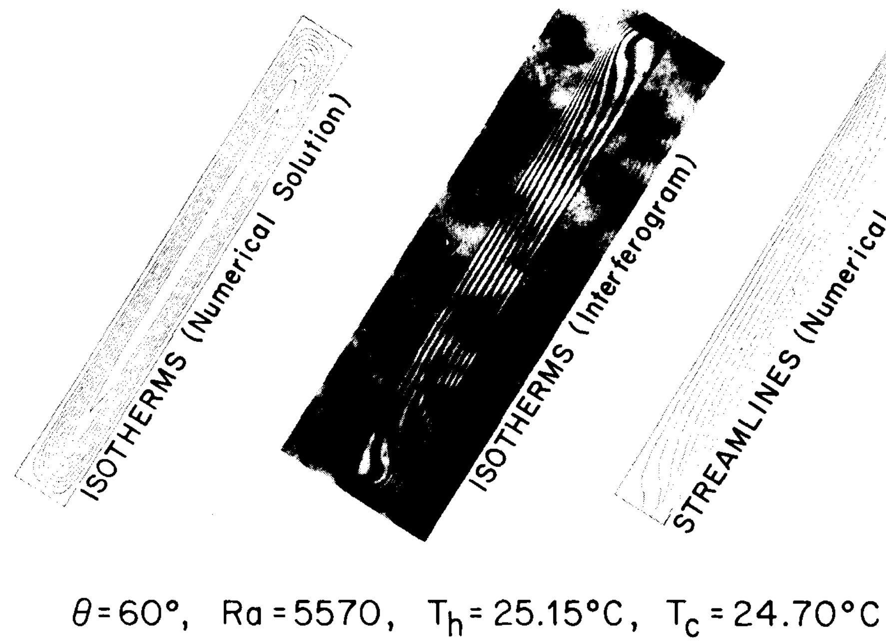

FIG. 2. Results of numerical solution compared to interferogram.

copper plates, each 25 cm (wide) by 15 cm (deep) by 3.18 cm (thick). Each plate is maintained at constant temperature by means of a water stream (passing through eight 1.27 cm by 1.27 cm channels cut in the inside of the copper plate) from a constant temperature circulator—a separate one used for each plate. The channels are connected to form a flattened double helix such that the flows in adjacent channels are in opposite directions to ensure uniformity of the plate temperature. An eight junction copper–constantan thermopile is used on each plate to measure the plate temperature.

The side walls of the test section are made of 1.27 cm Plexiglas. The test space filled with distilled water is bounded laterally by two spacers made of Plexiglas; they are hollow and filled with fiberglass. The ratio of heat flow passing through the spacers to total heat transfer passing through the water layer is typically about 0.002.

The test section rests on a mechanism capable of adjusting the inclination of the layer to the horizontal. The fluid layer is set from horizontal to vertical in intervals of 15°. To find the transition angle additional experiments are performed between 45° and 60°.

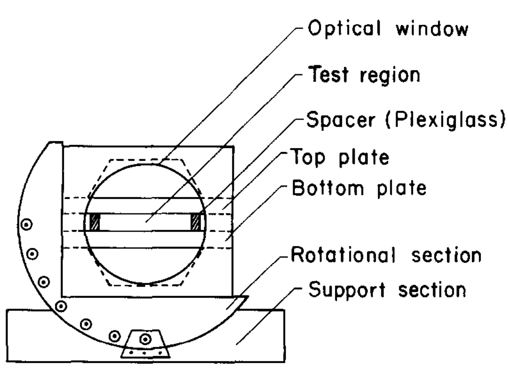

FIG. 3. Schematic diagram of test apparatus.

The University of Minnesota Heat Transfer Laboratory interferometer [18] with a He–Ne 5 MW laser light source is used to obtain the interferograms. The laser beam traverses the test section in the z-direction.

When measuring the critical Rayleigh number the temperature difference is first set at about 80% of the value corresponding to the estimated critical Rayleigh number [1] for each angle. Then the temperature difference is increased gradually by decreasing the temperature of the top plate or increasing the temperature of the bottom plate with an infinite fringe pattern in view. When the Rayleigh number passes the critical value, the isotherms become irregular. The spacing between isotherms in the center of the enclosure increases and the other isotherms are squeezed towards the two plates as the Rayleigh number is increased further. At sufficiently high Ra better defined longitudinal rolls appear to be present. The sensitivity of the method in determining Ra_{cr} is about $\pm 5\%$. An analysis of the interferograms yields the local temperature distribution and from this the temperature gradients at the surfaces of the plate. The local heat transfer coefficient can then be calculated using Fourier's law.

RESULTS AND DISCUSSION

Figures 4 and 5 show interferograms obtained in the present study. The dark and light lines are contours of

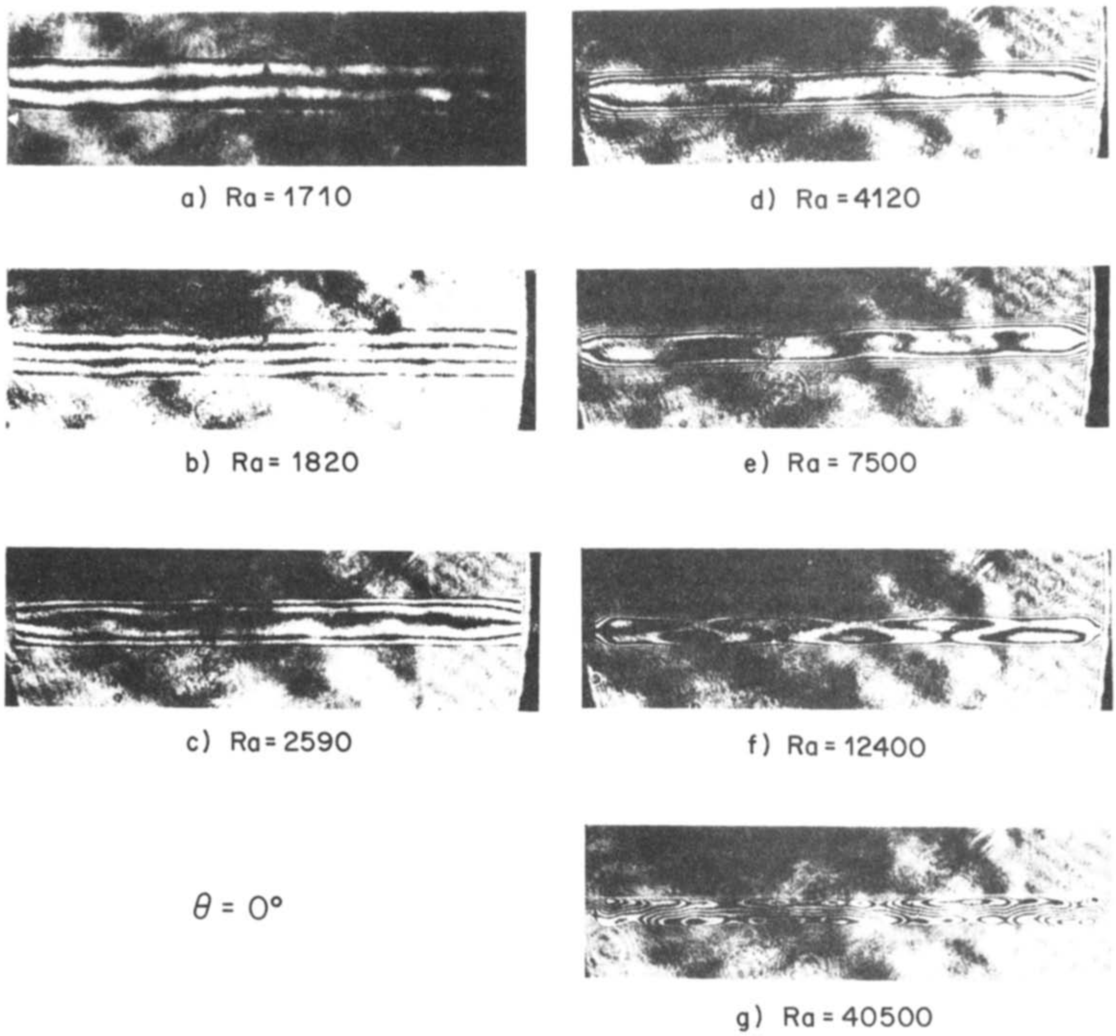

FIG. 4. Interferograms taken with horizontal layer heated from below.

constant optical path length. These approximate contours of constant average temperature along the direction of the laser beam. Figure 4 shows interferograms for a horizontal layer. At $Ra = 1710$ [Fig. 4(a)], the isotherms are straight horizontal and almost equally spaced across the layer; the heat transfer is by conduction. The isotherms become irregular when the critical Rayleigh number is passed [Fig. 4(b)]. As Ra is increased further, the isotherms are squeezed towards the two plates [Fig. 4(c)]; covective motion appears in the center region. Figure 4(d) appears to show a series of longitudinal rolls with axes parallel to the x-direction. The isotherms in the center of the enclosure have an Ω-shape at larger Ra [Fig. 4(e)]. This pattern which appears for $Ra \approx 7000$ in the present experiments could be related to Bénard cells. At the beginning, the flow pattern is somewhat unsteady. The rolls are separated into small cells with increasing Ra. Finally, a complex more or less steady pattern is observed [Fig. 4(g)] for $Ra = 40\,500$.

Figure 5 shows isotherm patterns at different angles of inclination for $Ra = 4080$–4360. When $\theta = 0°$, the flow pattern is apparently longitudinal rolls with axes parallel to the x-axis. When the angle is increased, different fringe (isotherm) patterns appear. The critical Rayleigh number is defined by the onset of the longitudinal rolls on the base flow; in Fig. 5(b) at $\theta = 15°$ the longitudinal rolls occupy most of the fluid layer. When the angle is increased further, the longitudinal rolls persist, but the region occupied by them gradually reduces. When an angle of 57.5° is attained, the flow pattern changes to what appears to be a unicellular transverse roll with its axis parallel to the z-direction. This flow pattern persists at large angles of inclination. For $\theta = 180°$ the isotherms are equally-spaced straight lines parallel to the two plates.

Table 1 and Fig. 6, show measured values of the critical Rayleigh number at different inclinations of the layer in the region of longitudinal rolls. As can be seen from Fig. 6 the values of the critical Rayleigh number determined in the present experiments are somewhat higher than Hart's results [1]. The present nominal aspect ratio is nearly three times smaller than that in ref. [1]. Due to the restraint of the side walls the transition angle decreases with decreasing nominal aspect ratio [8]. Moreover, the critical Rayleigh number is

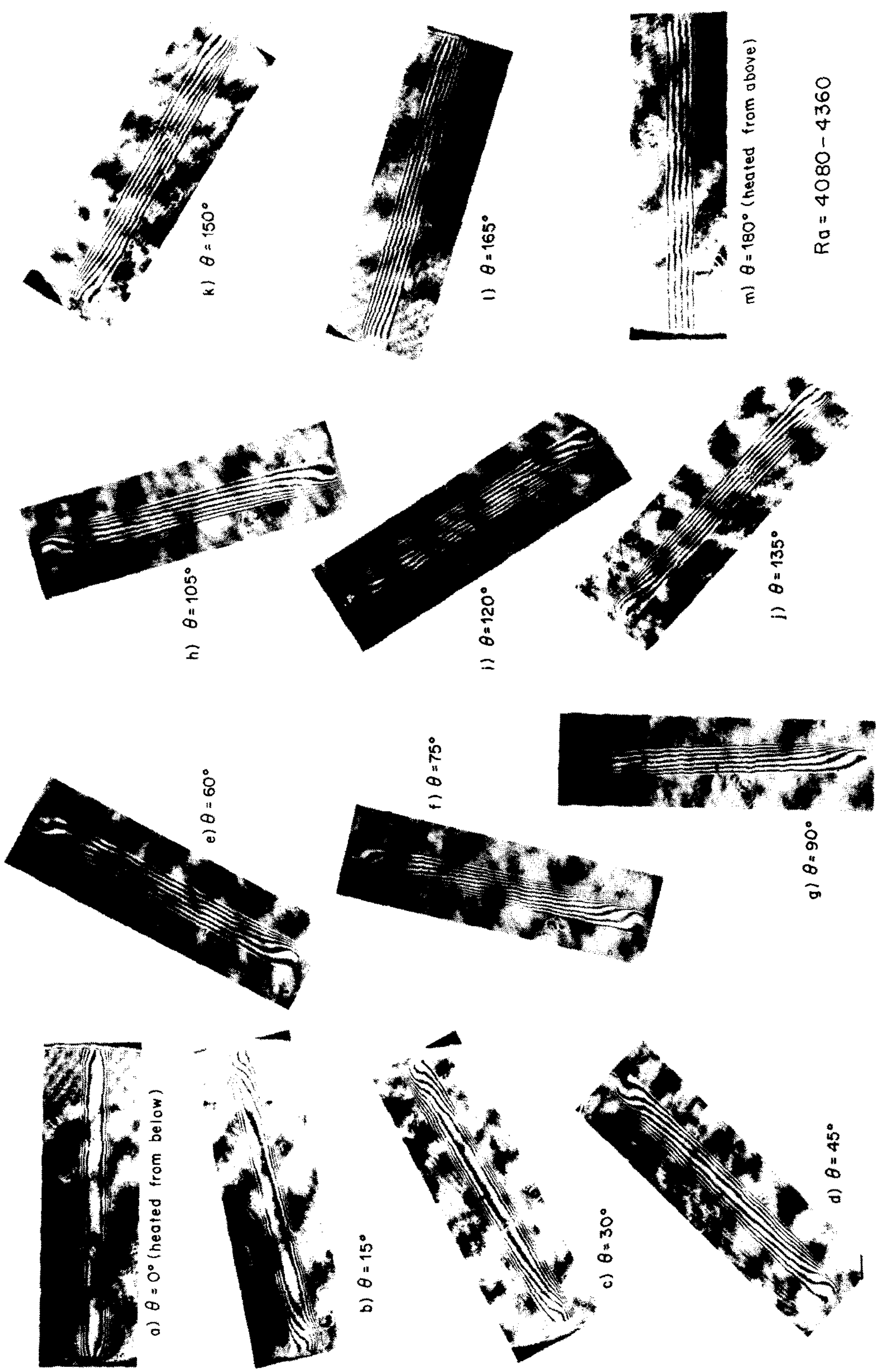

FIG. 5. Interferograms obtained with layer at different angles of inclination.

Table 1. Measured values of critical Rayleigh number

Angle, θ (deg.)	Ra_{cr}
0	1780 ± 60
15	2070 ± 80
30	2240 ± 80
45	3400 ± 160
50	4200 ± 220

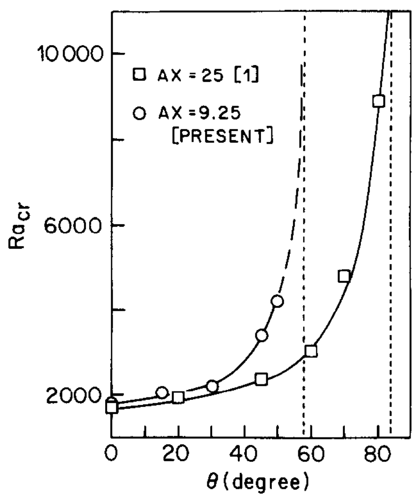

FIG. 6. Critical Rayleigh number as a function of angle of inclination.

increased when a fluid is constrained laterally [13]. Figure 7 shows a comparison of experimental results for transition angle. Table 2 lists the experimental conditions of different studies in which a nominal aspect ratio in the range of 7–9 was used. As can be seen, the studies obtained similar transition angles even though *Pr* and *Ra* were often quite different.

Linthorst *et al.* [9] indicate that the influence of *AZ* has been small in most experiments when the depth aspect ratio varied from 5 to 10. When $AX > 7$, and $AZ > 8$, the Prandtl and Rayleigh number apparently have no significant effect on the transition angle.

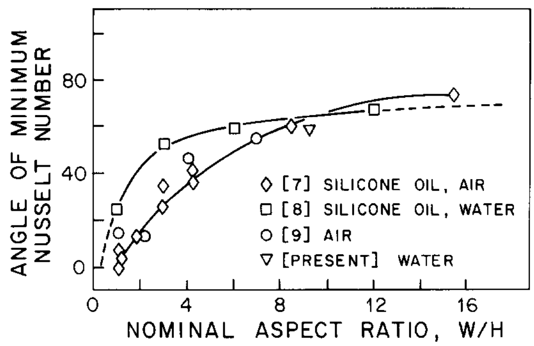

FIG. 7. Comparison of experimental results for transition angle.

When the nominal aspect ratio is varied from 1 to 5 the transition angle increases rapidly with increasing *AX*. In this region the experimental data obtained by different investigators have significant deviation (cf. Fig. 7). It appears that the boundary conditions, both thermal and flow, and the Prandtl number may have a significant influence on transition angle at small values of *AX*.

LOCAL HEAT TRANSFER

Figure 8 shows the variation of the local Nusselt number along the hot and cold plate surfaces. The maximum *Nu* appears near the starting (of the flow or effective boundary layer) corner and the minimum near the departure corner for both the hot and cold plate. At the starting corner of each plate, the temperature difference between the plate and the fluid coming from the opposite boundary is largest and the effective boundary layer is thinnest, hence, the maximum local values at that position. On the other hand, when the temperature difference is smallest and the boundary layer is the thickest, *Nu* is smallest. The magnitude and the variation of the local Nusselt number along each of the two (hot and cold) plates from the starting corner to the departure corner are almost the same for the conditions studied.

Note the difference in the variation of the local Nusselt number along the surfaces for the two inclinations. At $\theta = 60°$ the local Nusselt number

Table 2. Comparison of experimental conditions in studies of flow transition in inclined layer with $AX \sim 9$

	Transition angle (deg.)	Experimental conditions				
		AX	*AZ*	Medium	*Ra*	Side boundary condition
Ref. [7]	60	8.4	8.4	Air ($Pr = 0.71$)	3×10^3–1×10^5	Insulated
Ref. [8]	61	9*	9.87	Water ($Pr = 4.5$) and silicone oil ($Pr = 2000$)	1×10^4–1×10^6	Insulated
Ref. [9]	55	7	8	Air ($Pr = 0.71$)	5×10^3–2.5×10^5	Plexiglas
Present data	57.5	9.25	17.2	Water ($Pr = 6.3$)	1.7×10^3–1.7×10^4	Insulated

* Calculated from experimental data.

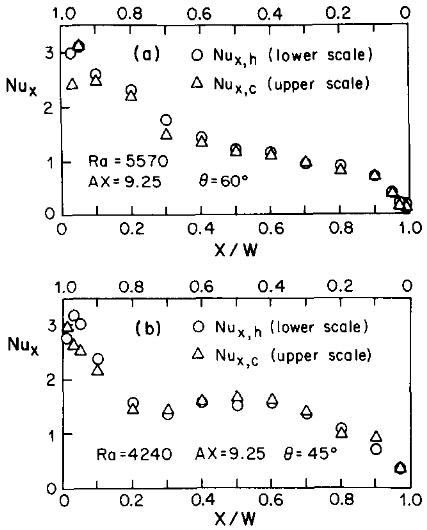

FIG. 8. Local Nusselt number along the hot and cold plate surfaces.

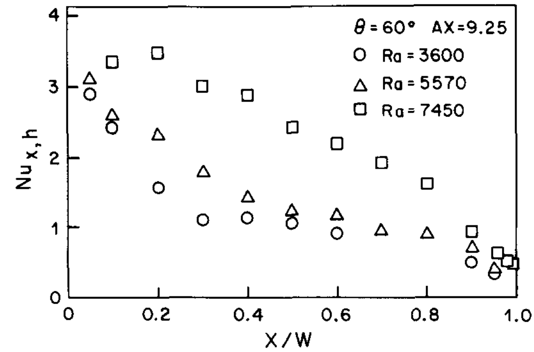

FIG. 10. Local Nusselt number along the hot plate surface for different Rayleigh numbers.

decreases monotonically with increasing X/W, but for $\theta = 45°$ the local Nusselt number decreases at first then increases with increasing X/W on the hot surface. A local maximum appears in the region of $X/W = 0.4 \sim 0.6$. The difference in the variation of heat transfer along the surface results from the different flow patterns at the different inclinations. For $\theta = 45°$ the mode of circulation in the region $X/W = 0.3 \sim 0.7$ is longitudinal rolls [Fig. 5(d)]. In this region isotherms are squeezed towards the plate surfaces yielding a local maximum of Nu in the central region of the plate.

Figure 9 shows the local Nusselt number on the hot plate surface for five angles of inclination. These coincide with some of the isotherm patterns shown in Fig. 5. Note that for $\theta = 180°$ the local Nusselt numbers are almost constant and equal to unity.

Figure 10 shows the local Nusselt number variations along the hot plate surface at $\theta = 60°$ for different Rayleigh numbers.

In Fig. 11 the experimental and computed local Nusselt numbers are compared for $\theta = 60°$. There is excellent agreement when the flow is basically 2-D, except in the region very close to the side walls on which the real boundary conditions are different from those assumed in the computation.

AVERAGE NUSSELT NUMBER

Average Nusselt numbers are determined through integration of the local Nusselt numbers over the plate surface. Table 3 summarizes the measured and calculated values of the average Nusselt number.

Clever [19] and Ruth *et al.* [20, 21] found that replacing Ra with $Ra(\cos\theta)$ would allow rescaling $\theta = 0°$ data to predict the average Nusselt number for $\theta < 60°$. For a near vertical layer, Ayyaswamy and Catton [22] and Raithby *et al.* [23] proposed that the average Nusselt number at $\theta = 90°$ be multiplied by $(\sin\theta)^{1/4}$ to obtain a prediction for other layer inclinations in the range $60° < \theta \leqslant 90°$.

For $\theta \leqslant 60°$ the average Nusselt number is plotted vs $Ra(\cos\theta)$, in Fig. 12. Also shown in this figure are results from other investigators. The present data are not too different from the predictions of refs. [12, 25].

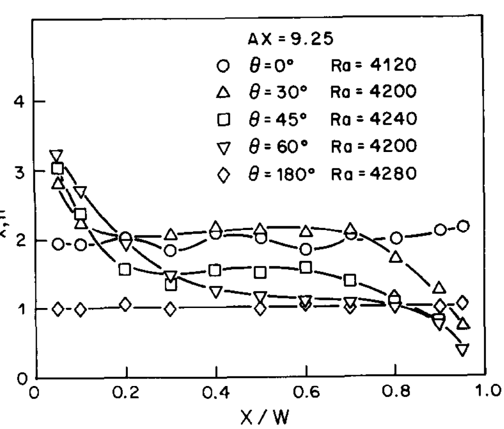

FIG. 9. Local Nusselt number along the hot plate surface for different angles of inclination.

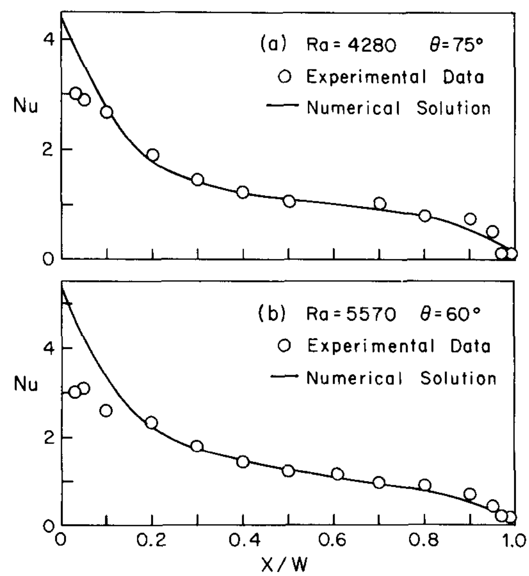

FIG. 11. Comparison between experimental and numerical determination of local Nusselt number.

Table 3. Average Nusselt number for heat transfer across inclined layer

θ (deg.)	Ra	$\overline{Nu}$ Experiment	Numerical solution
0	4120	1.953	
15	4240	1.88	
30	4200	1.56	
45	4240	1.483	
60	3600	1.306	1.259
60	4200	1.423	1.330
60	5570	1.481	1.443
60	7450	1.826	1.591
75	4280	1.331	1.36
90	4200	1.211	1.358
105	4080	1.182	1.324
120	4280	1.29	1.286
135	4160	1.101	1.204
150	4360	1.04	1.122
165	4270	0.98	1.03
180	4280	1.003	1.000

SUMMARY

Thermal instability and heat transfer by natural convection in a rectangular inclined water layer have been studied using interferometric techniques.

For $\theta = 0°$, the initial flow when the critical Rayleigh number is exceeded is in the form of longitudinal rolls aligned with the short horizontal dimension of the layer. When the Rayleigh number is further increased there is a break down of this flow and cells may appear. Near transition these cells are unsteady.

With respect to the angle of inclination two different preferred flow modes are observed. For $0° < \theta < 57.5°$, the flow is driven by local buoyancy variations and the preferred mode is longitudinal rolls superimposed on the base flow. For $57.5° \leqslant \theta < 180°$, the buoyancy leads to an overall hydrodynamic motion and a single transverse roll is present. The transition angle at which there is a crossover from one class of flow to the other is about 57.5° in the present tests.

From analysis of the interferograms, local and average Nusselt numbers are determined. Local Nusselt numbers along the hot and cold plates from starting corners to departure corners are similar. The local Nusselt numbers are a strong function of the angle of inclination.

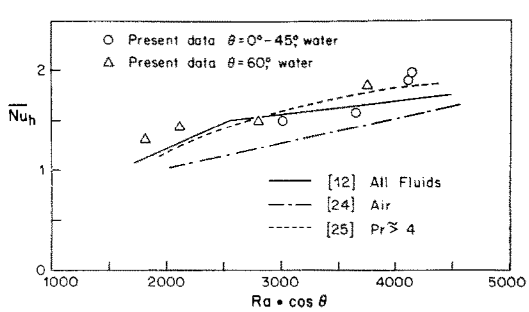

FIG. 12. Average Nusselt number as a function of Ra cos θ.

A numerical solution is carried out using a finite-difference scheme to predict the flow and temperature fields assuming 2-D natural circulation. Experimental and numerically computed values are in good agreement when the flow is in the form of a single roll.

Acknowledgements—This study was supported by a grant from the Heat Transfer Program of the National Science Foundation, Division of Mechanical Engineering and Applied Mechanics. H. D. Chiang contributed significantly to the final preparation of the manuscript.

REFERENCES

1. J. E. Hart, Stability of the flow in a differentially heated inclined box, *J. Fluid Mech.* **47**(3), 547–576 (1971).
2. K. G. T. Hollands and L. Konicek, Experimental study of the stability of differentially heated inclined air layers, *Int. J. Heat Mass Transfer* **16**, 1467–1476 (1973).
3. A. Pellow and R. V. Southwell, On maintained convective motion in a fluid heated from below, *Proc. R. Soc.* **176A**, 312–343 (1940).
4. I. Catton, The effect of insulating vertical walls on the onset of motion in a fluid heated from below, *Int. J. Heat Mass Transfer* **15**, 665–672 (1972).
5. H. Ozoe, H. Sayama and S. W. Churchill, Natural convection in an inclined square channel, *Int. J. Heat Mass Transfer* **17**, 401–406 (1974).
6. H. Ozoe, Natural circulation in an inclined rectangular channel heated on one side and cooled on the opposing side, *Int. J. Heat Mass Transfer* **17**, 1209–1217 (1974).
7. H. Ozoe, H. Sayama and S. W. Churchill, Natural convection in an inclined rectangular channel at various aspect ratios and angles—experimental measurements, *Int. J. Heat Mass Transfer* **18**, 1425–1431 (1975).
8. J. N. Arnold, I. Catton and D. K. Edwards, Experimental investigation of natural convection in inclined rectangular regions of differing aspect ratios, *Trans. Am. Soc. Mech. Engrs*, Series C, *J. Heat Transfer* **98**, 67–71 (1976).
9. S. J. M. Linthorst, W. M. M. Schinkel and C. J. Hoogendoorn, Flow structures with natural convection in inclined air-filled enclosures, *Trans. Am. Soc. Mech. Engrs*, Series C, *J. Heat Transfer* **103**, 535–539 (1981).
10. S. A. Korpela, A study of the effect of Prandtl number on the stability of the conduction regime of natural convection in an inclined slot, *Int. J. Heat Mass Transfer* **17**, 215–222 (1974).
11. S. M. Elsherbiny, K. G. T. Hollands and G. D. Raithby, Effect of thermal boundary conditions on natural convection in vertical and inclined air layers, *Trans. Am. Soc. Mech. Engrs*, Series C, *J. Heat Transfer* **104**, 515–520 (1982).
12. H. Buchberg, I. Catton and D. K. Edwards, Natural convection in enclosed spaces—a review of application to solar energy collection, *Trans. Am. Soc. Mech. Engrs*, Series C, *J. Heat Transfer* **98**, 182–188 (1976).
13. I. Catton, Natural convection in enclosures, *Proc. 6th Int. Heat Transfer Conf.*, Toronto, Canada, Vol. 6, pp. 13–31 (1978).
14. S. M. Elsherbiny, G. D. Raithby and K. G. T. Hollands, Heat transfer by natural convection across vertical and inclined air layers, *Trans. Am. Soc. Mech. Engrs*, Series C, *J. Heat Transfer* **104**, 96–102 (1982).
15. D. Dropkin and E. Somerscales, Heat transfer by natural convection in liquids confined by two parallel plates which are inclined at various angles with respect to the horizontal, *Trans. Am. Soc. Mech. Engrs*, Series C, *J. Heat Transfer* **87**, 77–82 (1965).
16. S. Acharya and R. J. Goldstein, Natural convection in an externally vertical or inclined square box containing internal energy sources, in *Natural Convection in Enclosures*, Vol. 26, pp. 17–26. ASME HTD (1983).

17. S. V. Patankar, *Numerical Heat Transfer and Fluid Flow*. Hemisphere, Washington, DC (1980).
18. R. J. Goldstein, Optical measurement of temperature, in *Measurements in Heat Transfer* (edited by E. R. G. Eckert and R. J. Goldstein) (2nd edn.). McGraw-Hill, New York (1970).
19. R. M. Clever, Finite amplitude longitudinal convection rolls in an inclined layer, *Trans. Am. Soc. Mech. Engrs*, Series C, *J. Heat Transfer* **95**, 407–408 (1973).
20. D. W. Ruth, K. G. T. Hollands and G. D. Raithby, On free convection experiments in inclined air layers heated from below, *J. Fluid Mech.* **96**, 459–479 (1980).
21. D. W. Ruth, G. D. Raithby and K. G. T. Hollands, On the secondary instability in inclined air layers, *J. Fluid Mech.* **96**, 481–492 (1980).
22. P. Ayyaswamy and I. Catton, The boundary-layer regime for natural convection in a differentially heated tilted rectangular cavity, *Trans. Am. Soc. Mech. Engrs*, Series C, *J Heat Transfer* **95**, 543–545 (1973).
23. G. D. Raithby, K. G. T. Hollands and T. Unny, Analysis of heat transfer by natural convection across vertical fluid layers, *Trans. Am. Soc. Mech. Engrs*, Series C, *J. Heat Transfer* **99**, 287–293 (1977).
24. K. G. T. Hollands, T. E. Unny, G. D. Raithby and L. Konicek, Free convective heat transfer across inclined air layers, *Trans. Am. Soc. Mech. Engrs*, Series C, *J. Heat Transfer* **98**, 189–193 (1976).
25. G. D. Raithby and K. G. T. Hollands, Natural convection, in *Handbook of Heat Transfer* (2nd edn.), to be published.

UNE ETUDE INTERFEROMETRIQUE DE LA CONVECTION NATURELLE DANS UNE COUCHE D'EAU INCLINEE

Résumé—L'instabilité thermique et le transfert de chaleur par convection naturelle sont étudiés par interférométrie dans une couche d'eau inclinée et rectangulaire aux faibles nombres de Rayleigh. On observe les modes d'écoulement préférentiels à différents angles d'inclinaison (θ) par rapport à l'horizontale. Pour $0° < \theta < 57{,}5°$, le mode est à rouleaux longitudinaux superposés à l'écoulement de base. Pour $57{,}5° < \theta < 90°$, on observe un seul rouleau bidimensionnel. Les nombres de Nusselt locaux et moyens sont comparés aux solutions numériques obtenues en supposant un rouleau transversal bidimensionnel.

EINE INTERFEROMETRISCHE UNTERSUCHUNG DER FREIEN KONVEKTION IN EINER GENEIGTEN WASSERSCHICHT

Zusammenfassung—Mit Hilfe eines Interferometers wurden die thermische Instabilität und die Wärmeübertragung bei freier Konvektion in einer geneigten rechteckigen Wasserschicht bei kleinen Rayleighzahlen untersucht. Abhängig von den unterschiedlichen Neigungswinkeln bezüglich der Horizontalen (θ) wurden die verschiedenen sich einstellenden Strömungsarten beobachtet. Für $0° < \theta < 57{,}5°$, sind longitudinale Rollwirbel, die sich der Grundströmung überlagern, vorherrschend. Für $57{,}5° \leqslant \theta \leqslant 90°$ wurde ein einzelner zweidimensionaler Wirbel beobachtet. Gemessene örtliche und mittlere Nusselt-Zahlen werden mit numerischen Ergebnissen verglichen, wobei ein zweidimensionaler querliegender Wirbel der Rechnung zugrunde gelegt wurde.

ИНТЕРФЕРОМЕТРИЧЕСКОЕ ИССЛЕДОВАНИЕ ЕСТЕСТВЕННОЙ КОНВЕКЦИИ В НАКЛОННОМ СЛОЕ ВОДЫ

Аннотация—На интерферометре проведены исследования конвективной неустойчивости и теплопереноса естественной конвекцией в наклонном прямоугольном слое воды при малых значениях числа Рэлея. При различных углах наклона слоя к горизонтальному положению (θ) наблюдаются различные режимы течения. В диапазоне $0° < \theta < 57{,}5°$ предпочтительной структурой является течение с продольными валами на фоне основного течения. В диапазоне $57{,}5° \leq \theta \leq 90°$ наблюдается единичный двумерный вал. Проведено сравнение измеренных местных и средних значений числа Нуссельта с результатами численных расчетов, проведенных для двумерного поперечного вала.